

Enhancing the mechanical properties of epoxy resin by addition of an amino-terminated hyperbranched polymer grown on glass fiber

Shuiping Li^{1,2} · Chong Cui²

Received: 6 August 2015 / Accepted: 7 October 2015 / Published online: 15 October 2015
© Springer Science+Business Media New York 2015

Abstract In this study, glass fiber (GF) was grafted by an amino-terminated hyperbranched polymer (ATHBP). The structure of GF-ATHBP was characterized by attenuated total internal reflectance infrared spectroscopy, ¹H nuclear magnetic resonance spectroscopy, thermal gravimetric analysis, and field emission scanning electron microscopy (FESEM). The modified GFs were used to produce high-performance epoxy composites. The effects of GF-ATHBPs on the mechanical properties of composites were investigated, discussing the results from tensile, flexural, and impact tests. The results showed that the grafting ratio of ATHBP on GF was 7.6 %, and the thickness of ATHBP layer was about 1.9 μm. And the incorporation of GF-ATHBPs could favorably improve the mechanical properties of epoxy resins. FESEM morphologies showed that the excellent compatibility and interaction may be associated with the great enhancement of mechanical properties of epoxy/GF-ATHBP composites.

Introduction

Epoxy resins, which exhibit superior engineering properties such as high tensile strength and flexible strength, high stiffness and modulus, great adhesion, low creep, low shrinkage on

cure, excellent chemical and corrosion resistance, and good thermal and electrical properties, are important thermosetting polymers [1–3]. Unfortunately, the high crosslinking density of the cured network is closely associated with poor impact resistance [4, 5]. Because of high strength and stiffness per unit weight, glass fiber and carbon fiber are incorporated into epoxy matrixes to improve the mechanical properties and also the toughness [3, 6–17]. Fiber-reinforced epoxy composites (FRECs) have been widely used in various applications such as aerospace, aircraft, defense, sporting goods, wind turbine, marine, automobile, boat, and mechanical and electronic applications [7, 18, 19] due to their high specific stiffness and strength, good dimensional stability, great modulus, low density, low creep, low dielectric constant, excellent flexural strength and tensile strength, ease of processability, and relatively low costs [6, 20, 21]. The properties of FRECs are significantly dependent on the properties of composite constituents such as epoxy matrix, fiber, and the interface between them [7, 22, 23]. However, the notable disadvantage of fiber is its weak combination with epoxy matrix [8, 24–27]. Due to this nature, an incompatibility between the fiber and the matrix exists which decreases the properties of the composite. This defect can be overcome by chemical modification of fiber surface so as to make it a strong adhesive [28–33].

Hyperbranched polymers (HBPs) are a kind of interesting materials due to their low melting points and viscosities, high-density and versatile terminal groups, and unique spherical structure. The use of suitable terminal groups, such as hydroxyl, epoxide, amine, and carboxylic groups, can enhance the compatibility between HBPs and polymer matrixes [34]. Thus, HBPs are used as a new class of modifiers for epoxy resins [35–37]. The advantages that the introduction of HBP into epoxy matrix are their high-density and versatile terminal functional groups, a lot of

✉ Chong Cui
cuichongnust@163.com

¹ School of Materials Engineering, Yancheng Institute of Technology, Yancheng 224051, Jiangsu, People's Republic of China

² College of Materials Science and Engineering, Nanjing University of Science and Technology, Nanjing 210094, Jiangsu, People's Republic of China

free spaces and free volumes in their structures [38, 39], and their peculiar structures [39–41].

The novelty of the present work is the use of a novel modified glass fiber (GF) grafted by amino-terminated hyperbranched polymer (ATHBP) in two-step polycondensation, as a filler for an epoxy resin. In this study, firstly GF was treated by a silane coupling agent, then hyperbranched polymer with hydroxyl groups (HBPH) was grown on the surface of GF, and lastly GF-HBPH was terminated by polyamines. The mechanical properties of epoxy/GF composites were studied, discussing the results from tensile, flexural, and impact tests. Field emission scanning electron microscope (FESEM) was used to examine the fracture surfaces of composites to discuss the toughening mechanism.

Experiment sections

Materials

Diglycidyl ether of bisphenol-A epoxy resin E51, which has an epoxide equivalent of 185–208 g/eq, was obtained from Hangzhou Wujingang Adhesive Co., Ltd, Hangzhou, China. A general hardener (polyamide 650), which has an amine value of 220 ± 20 mgKOH/g, was supplied by Wuxi Resin Factory, Wuxi, China. GFs, with an average length of 30 μm and diameter of 10 μm , were purchased from Corker CO., LTD, Taikang, China. γ -Aminopropyl triethoxysilane (γ -APS, KH-550) was purchased from Sinopharm Chemical Reagent Co., Ltd, Shanghai, China. Succinic anhydride, diethanolamine, aqueous solution of H_2O_2 (30 wt%), diethylenetriamine (DETA), and *N,N*-dimethylacetamide (DMA) were purchased from Chengdu Kelong Chemical Reagent Company, Chengdu, China.

Fabrication of glass fiber grafted by amino-terminated hyperbranched polymer (GF-ATHBP)

The process was similar to our former reports [35, 37]. Typically, GFs were first treated with an aqueous solution of H_2O_2 and a kind of silane coupling agent, γ -APS. After dried under vacuum at 80 $^\circ\text{C}$ for 24 h, 1 g GFs were added into the mixture of 1.57 g succinic anhydride and 1.5 g diethanolamine at 70 $^\circ\text{C}$ for 2 h and then heated to 120 $^\circ\text{C}$ for 6 h. Then the temperature was decreased to 110 $^\circ\text{C}$, and 3.1 g DETA was added dropwise into the mixture under stirring for 10 h. After washed and filtered three times with DMA and dried under vacuum at 80 $^\circ\text{C}$ for 12 h, GF-ATHBP was obtained. The chemical structure of GF-ATHBP is shown in Scheme 1.

Preparation of epoxy/GF composites

Epoxy and GF-ATHBP (GF-ATHBP/epoxy, 0–5 wt/wt%) were blended and sonicated for 10 min. Then polyamide 650 (epoxy/polyamide 650, 1:1.2 wt/wt), which was preheated to 60 $^\circ\text{C}$, was added and the resulting mixture was stirred for another 10 min. Finally, the mixture was poured into stainless steel templates and cured at 60 $^\circ\text{C}$ for 48 h for testing in an oven. The whole preparation process is shown in Scheme 2.

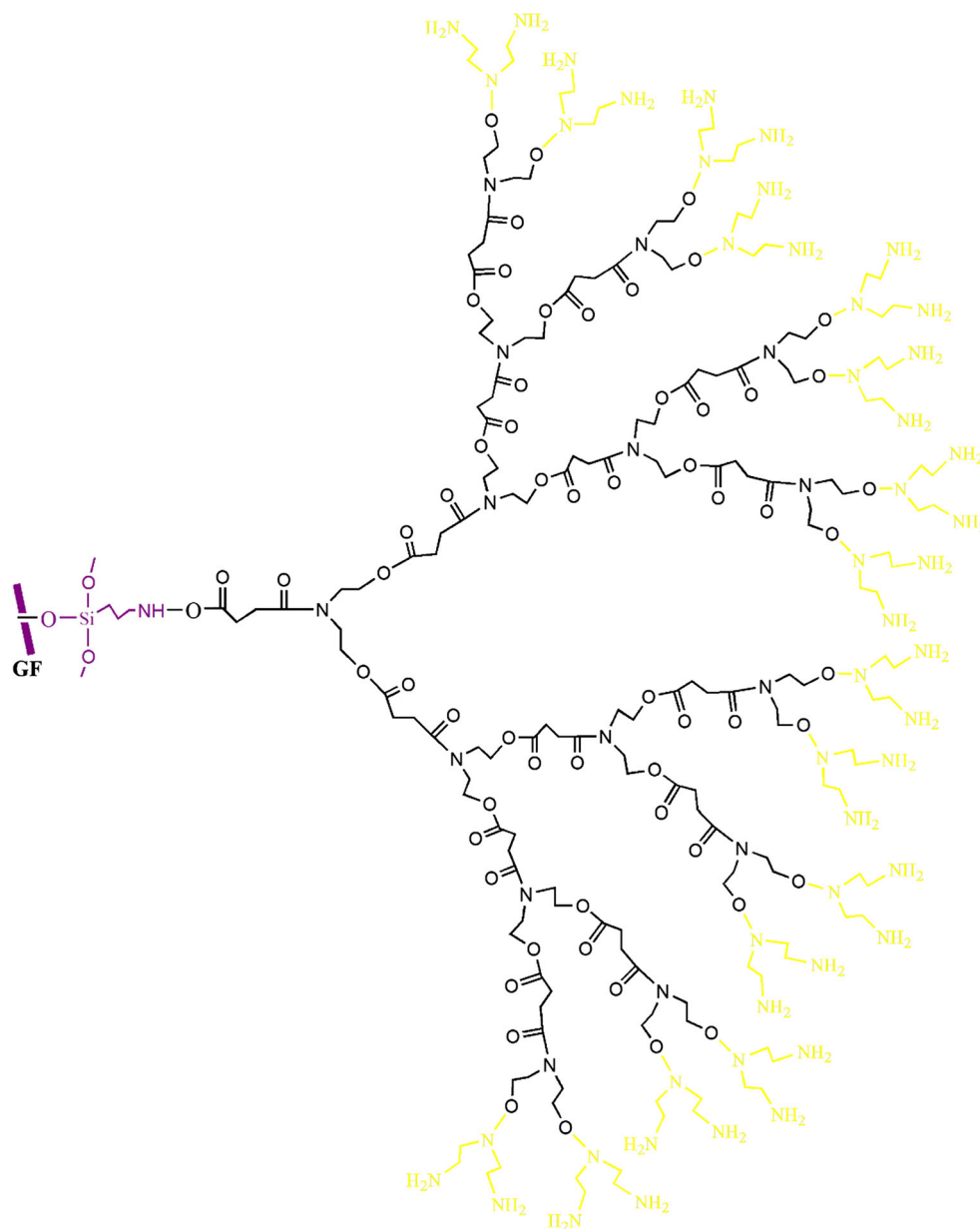
Characterization

Attenuated total internal reflectance infrared (ATR-IR) spectroscopic analysis was conducted with a Tensor 37 instrument (Bruker, Germany) within the range of 400–4000 cm^{-1} and a resolution of 4 cm^{-1} . ^1H nuclear magnetic resonance (^1H NMR) spectrum was recorded on an AVANCE 500 NMR spectrometer (Bruker, Switzerland) with deuterated dimethyl sulfoxide (DMSO-d_6) as the solvent at 293 K. Thermal gravimetric analysis (TGA) was performed with a SHIMADZU DTG 60 TG/DTA simultaneous measuring instrument (SHIMADZU, Japan) at a heating rate of 20 $^\circ\text{C min}^{-1}$ from 30 to 800 $^\circ\text{C}$ under a nitrogen atmosphere. Tensile tests were performed with an SHIMADZU AG-X plus (SHIMADZU, Japan) test machine. The composite samples were prepared according to GB/T 2567-2008. Flexural tests were characterized with a UTM4000 electromechanical universal testing machine (SANS, China) according to GB/T 2567-2008 standard of dimensions 80 * 15 * 4 mm. Impact resistance measurements were performed with an ZBC 50 pendulum impact testing machine (New SANS, China) without a notch in the specimen according to GB/T 2567-2008 standard of a thickness of 4 mm and a width of 10 mm. Field emission scanning electron microscopy (FESEM) images were recorded using a Hitachi SU8000 field emission scanning electron microscope (Hitachi, Japan), and the fracture surfaces of the composites were sputter-coated with gold before observation.

Results and discussions

Characteristics of the GF-ATHBP

The ATR-IR spectrum of GF-ATHBP is shown in Fig. 1. The broad peak at 3295.9 cm^{-1} is ascribed to the symmetric stretching of $-\text{NH}$. The two weak peaks at 2943.5 and 2842.1 cm^{-1} are attributed to the C–H stretching. The strong peak at 1647.8 cm^{-1} is assigned to the C=O stretching. The weak peak at 1554.8 cm^{-1} is attributed to the N–H bending vibration. The peak at 1434.8 cm^{-1}

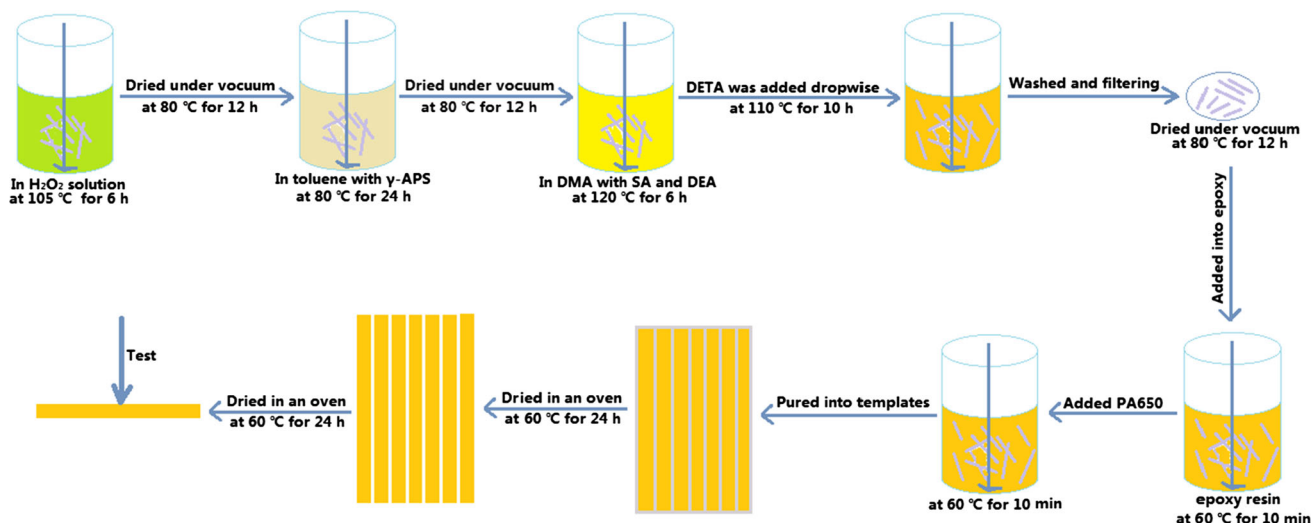
Scheme 1 The chemical structure of GF-ATHBPs

belongs to the C–H bending vibration. The weak peak at 1267.5 cm^{-1} is ascribed to the C–O–C stretching vibration. The strong peak at 1063.8 cm^{-1} is assigned to the C–N stretching. These peaks indicate that ATHBP may be successfully grafted onto the surface of silanized GFs.

NMR spectroscopy can provide detailed information about the structure, dynamics, reaction state, and chemical environment of molecules. The ^1H NMR spectrum of GF-ATHBP is shown in Fig. 2. As can be seen in Fig. 2, the ^1H NMR spectrum clearly displays the characteristic peaks of ATHBP, the peaks appearing at 1.779 ppm (N–CH₂–CH₂–O, protons a), 2.533 ppm (N–CH₂–CH₂–O, protons b), 2.188 ppm (C–CH₂–CH₂–, protons c), 2.665 ppm (CH₂–CH₂–C, protons d), 3.222 ppm (N–CH₂–CH₂–N, protons e),

3.414 ppm (N–CH₂–CH₂–N, protons f), 1.554 ppm (N–CH₂–CH₂–NH₂, protons g), 3.503 ppm (N–CH₂–CH₂–NH₂, protons h), and 7.933 ppm (N–CH₂–CH₂–NH₂, protons i). And the spectrum shows three kinds of proton peaks, which can be attributed to linear, dendritic, and terminal units. For instance, the peaks at 1.779, 2.533, 2.188, and 2.56 ppm are attributed to the linear units, the peaks at 3.222 and 3.414 ppm are assigned to the dendritic units, and the peaks at 1.554, 3.503, and 7.933 ppm are ascribed to the terminal units.

TGA is commonly used to determine selected characteristics of materials that exhibit either mass loss or gain due to decomposition, oxidation, or loss of volatiles (such as moisture). Figure 3 shows the TGA curves of hydroxylated GF, silanized GF, ATHBP, and GF-ATHBP



Scheme 2 The routes of synthesis of GF-ATHBP and fabrication of composite

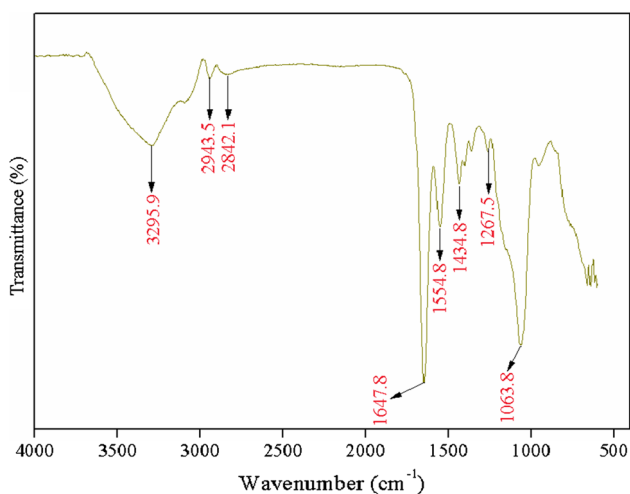


Fig. 1 ATR-IR spectrum of GF-ATHBP

measured under nitrogen atmosphere. As the weight loss diagrams illustrate, the final weight losses of hydroxylated GF, silanized GF, ATHBP, and GF-ATHBP at 800 °C are 18.6, 33.4, 77.3, and 50.5 %, respectively. Thus, the grafting ratio of silane on GF is 14.8 %. Furthermore, the temperature for 5 and 10 wt% weight losses ($T_{5\%}$ and $T_{10\%}$) of silanized GFs is 103.8 and 223.2 °C, respectively. In contrast, the GF-ATHBP is stable until 200 °C and no meaningful weight loss is detected. The $T_{5\%}$ and $T_{10\%}$ values of GF-ATHBP are 229.3 and 320.7 °C, respectively. The higher decomposition temperature of GF-ATHBP may be due to that the grafted ATHBP reduces the moisture content owing to hydrophobicity on the surface of GFs [42]. However, the presence of ATHBP makes GF-ATHBP to be less stable than silanized GF under high temperature. As the weight loss diagram of GF-ATHBP

illustrates, the GF-ATHBP has a higher weight loss at 800 °C than the corresponding sample of silanized GF. It should be noticed that the weight loss of ATHBP increases slowly after 600 °C, which indicates that ATHBP decomposes completely at that temperature. The weight losses of GF-ATHBP and silanized GF at 600 °C are 37.1 and 29.5 %, respectively. So the grafting ratio of ATHBP on GF is 7.6 %. The TGA curves confirm the ATHBP molecules being successfully attached to the surface of the silanized GF.

Figure 4 shows the surface characterizations of the silanized GFs and GF-ATHBPs. The surfaces of silanized GFs are rough and the average diameter is about 11.3 μm (Fig. 4a), calculated from the inset image with high magnification. The surfaces of GF-ATHBPs, which are shown in Fig. 4b, are rougher than those of silanized GFs. And the average diameter is about 13.2 μm , which is calculated according to the inset image of a single GF-ATHBP in Fig. 4b. The diameter change, about 1.9 μm , may be another evidence to indicate the successful growth of ATHBP onto the surfaces of GF.

Mechanical properties of composites

The tensile strength of epoxy/GF composites as a function of GF content is presented in Fig. 5. Compared to the silanized GFs, the tensile strength of the composites in the presence of GF-ATHBPs steadily enhances with increase of GF-ATHBPs content. As can be seen from Fig. 5, the highest tensile strength is 49.43 MPa, obtained for 2 wt% GF-ATHBPs, which is 31.1 % higher than that of the neat epoxy. With further addition of GF-ATHBPs, the tensile strength reduces dramatically and even becomes the lowest when it reached 5 wt% loading. The tensile modulus of the

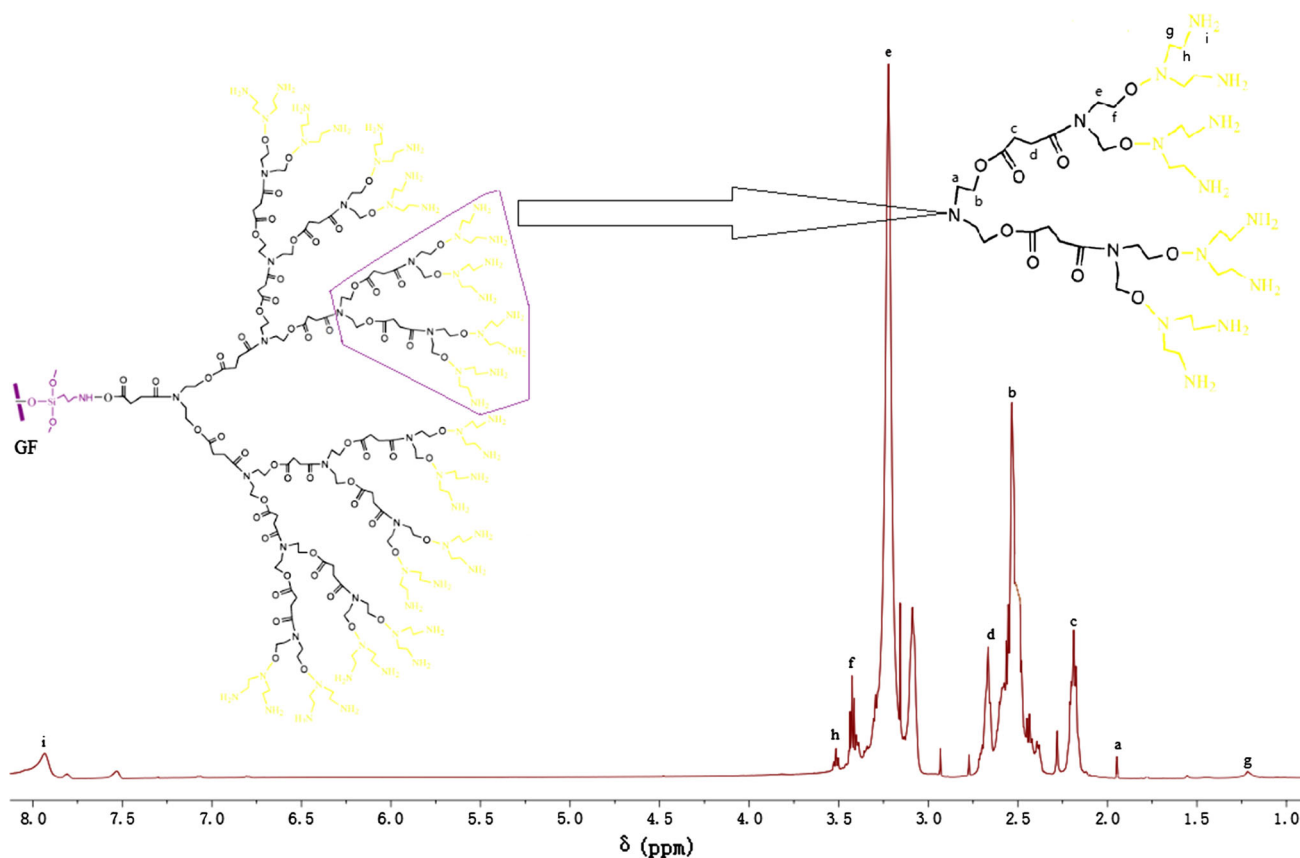


Fig. 2 ¹H NMR spectrum of GF-ATHBP

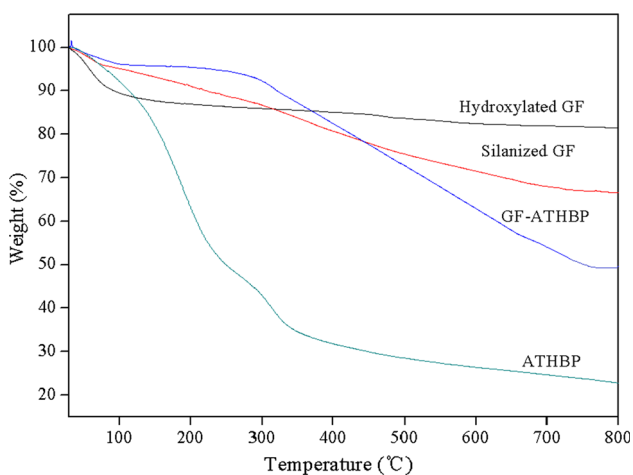


Fig. 3 TGA curves of hydroxylated GF, silanized GF, ATHBP, and GF-ATHBP

neat epoxy and epoxy composites is shown in Fig. 6. The change in the trend of the tensile modulus graph is similar to the tensile strength graph. The tensile modulus increases steadily from 1571 MPa for neat epoxy to 2427 MPa for composite with 2 wt% GF-ATHBPs, corresponding to the increase of 54.4 %; after that, the trend alters and decreases

to 1496 MPa for composite with 5 wt% GF-ATHBPs. Similar to the effect of GF-ATHBPs, the tensile modulus increases with the increase of silanized GF content, reducing the increasing trend. But the increase in epoxy composite modified with silanized GF is lower than that in the composite with same content of GF-ATHBP. Elongation at break is another index to evaluate the tensile property of epoxy-based composites and is shown in Fig. 7. It can be seen from Fig. 6, the elongation at break increases sharply from 2.43 % for the neat epoxy to 5.24 % for the composite with 2 wt% GF-ATHBPs, increasing by about 115.6 %. And then the trend alters and the elongation value decreases to 2 % for 5 wt% GF-ATHBPs. In contrast, the elongation at break is independent on the addition of silanized GFs except the formulation with 1 wt% GFs. The growth of ATHBP has affected the affinity between GFs and epoxy matrixes effectively, leading to a better dispersion of GFs and also improving the compatibility and interaction between GFs and epoxy matrixes.

The flexural strength of composites with different contents of GFs is shown in Fig. 8. Similar to the results of tensile test, the flexural strength increases with the increase of GF-ATHBP content, reducing the increasing trend. The highest flexural strength is 92.34 MPa, obtained for 2 wt%

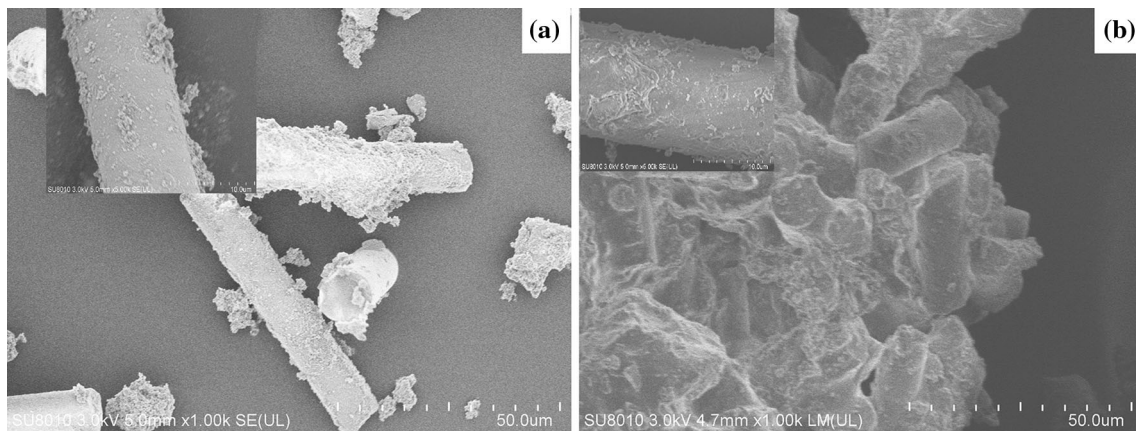


Fig. 4 FESEM images of silane-functionalized GFs (a) and GF-ATHBPs (b)

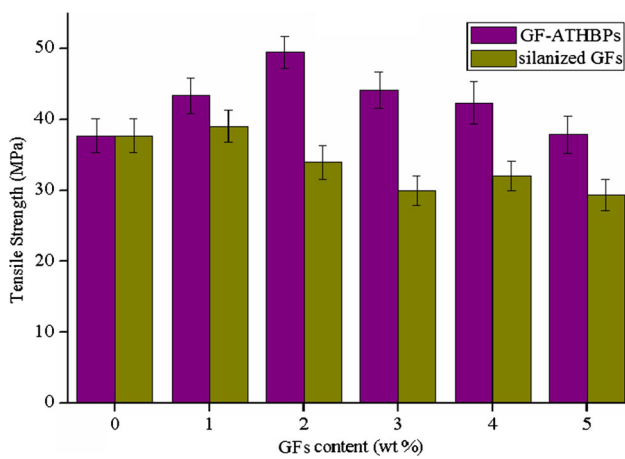


Fig. 5 Tensile strength of composites as a function of GF content

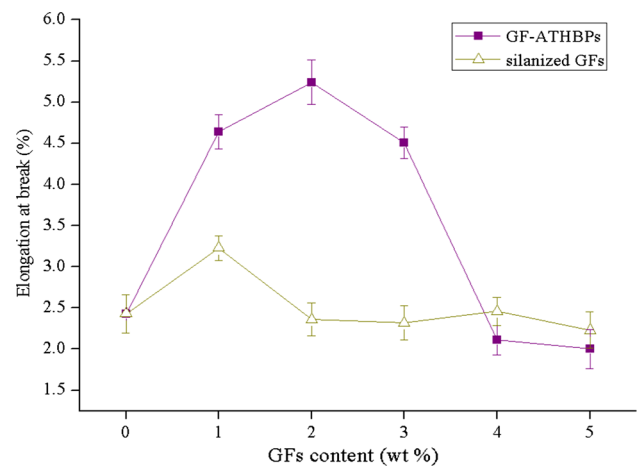


Fig. 7 Elongation of composites as a function of GF content

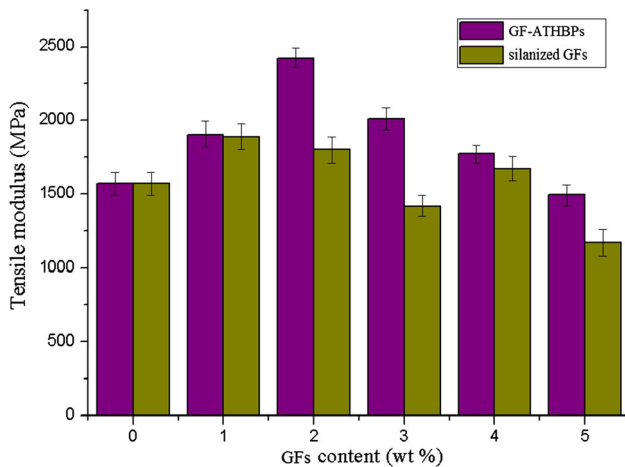


Fig. 6 Tensile modulus of composites as a function of GF content

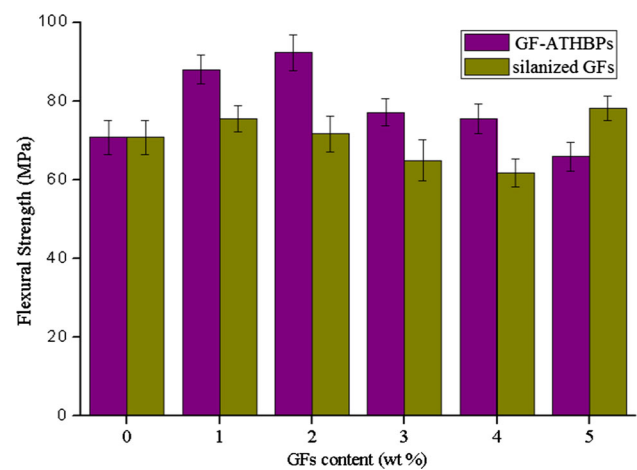


Fig. 8 Flexural strength of composites as a function of GF content

GF-ATHBPs, which is 30.5 % higher than that of the neat epoxy. It also can be observed that the effect of silanized GFs on the flexural strength is less obvious than that of

GF-ATHBPs and it is difficult to summarize the patterns. Figure 9 shows the impact strength of composites as a function of GF content. As can be seen from Fig. 9, the

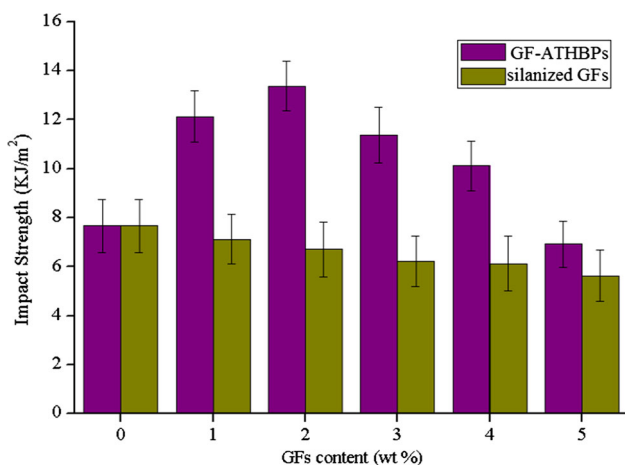


Fig. 9 Impact strength of composite as a function of GF content

impact strength suddenly increases from 7.667 kJ/m^2 for the neat epoxy to 13.375 kJ/m^2 for the composite with 2 wt% GF-ATHBPs, which increases by about 74.4 %. Then it starts to decrease after the loading exceeds 2 wt%. Generally, this phenomenon occurs with an inhomogeneous distribution, while the quantity of GF-ATHBPs increases. The results of impact tests can be explained as follows: firstly, grafted GFs perform a better improving effect at lower loading due to their enhanced compatibility and interaction with epoxy matrixes. The former may optimize the distribution, whereas the latter may guarantee an effective stress transfer from the matrixes to the GF-ATHBPs [43]. Secondly, the incorporation of GF-ATHBPs may decrease the crosslinking density of epoxy composite, which is due to that the growth of ATHBP breaks the stoichiometric balance between epoxide and amine values and then leads to the excess of curing agents. Lastly, an inhomogeneous distribution and self aggregation cause negative effects on the mechanical properties of composites. The impact strength of composites decreases with increasing silanized GF content. On the whole, ATHBP is helpful for our epoxy-based composites by improving GF dispersion, compatibility, and interfacial interaction and thus gives remarkable improvements on mechanical properties.

Morphologies of GF-ATHBPs and the impact fracture surfaces of composites

The change in mechanical properties can possibly be explained by observing the differences in the impact fracture surfaces of the specimens. The impact fracture surface morphologies of specimens are shown in Fig. 10. The neat epoxy shows a typical smooth surface with a little crack propagation (Fig. 10a), which leads to poor resistance to

mechanical damage, especially for impact resistance. The fracture surface image of composite with silanized GFs shows several large shearing deformations (Fig. 10b), which may be attributed to the improvement in the mechanical properties. However, the smooth surface of GF, which indicate the poor compatibility between GFs and epoxy matrixes, may be the weaknesses of composites and thus decreases the mechanical properties. The impact fracture surface images of composites with GF-ATHBPs (Fig. 10c, d) show more crack propagations, crack deflections, and shearing deformations, which support the improved mechanical properties. Moreover, the surface of exposed GF-ATHBP is rough and the exposed part is short, which indicate the excellent compatibility and strong interaction between GF-ATHBP and epoxy matrix. Furthermore, the embedded part of GF-ATHBP can transfer stress from GF-ATHBP to the epoxy matrix and thus improve the mechanical properties.

Conclusions

GF, grafted by an ATHBP, named as GF-ATHBP, was incorporated into epoxy resin to fabricate epoxy-based composites. The structure of GF-ATHBP was characterized by ATR-IR, ^1H NMR, TGA, and FESEM. The effects of GF-ATHBP content on the mechanical properties of composites were studied, discussing the results from tensile, flexural, and impact tests. For comparison, composites with silanized fibers were also fabricated and investigated. The impact fracture surfaces of composites were observed by FESEM to explain the change in the mechanical properties.

The results of ATR-IR and ^1H NMR indicate the successful growth of ATHBP onto the surfaces of GFs. TGA curves illustrate that the grafting ratio is about 7.6 %. FESEM images show that the grafting layer on the surface of GF is about $1.9 \mu\text{m}$.

Compared to the neat epoxy and composites with silanized GFs, the introductions of GF-ATHBPs can favorably improve the mechanical properties of epoxy-based composites. For instance, the tensile strength, elongation at break, flexural strength, and impact strength for the composite with 2 wt% GF-ATHBPs increase by about 31.1, 115.6, 30.5, and 74.4 %, compared to the neat epoxy, respectively.

FESEM morphologies show that the excellent compatibility and interaction between GF-ATHBP and epoxy matrix may be ascribed to the enhancement of mechanical properties of epoxy/GF-ATHBP composites, especially for impact strength.

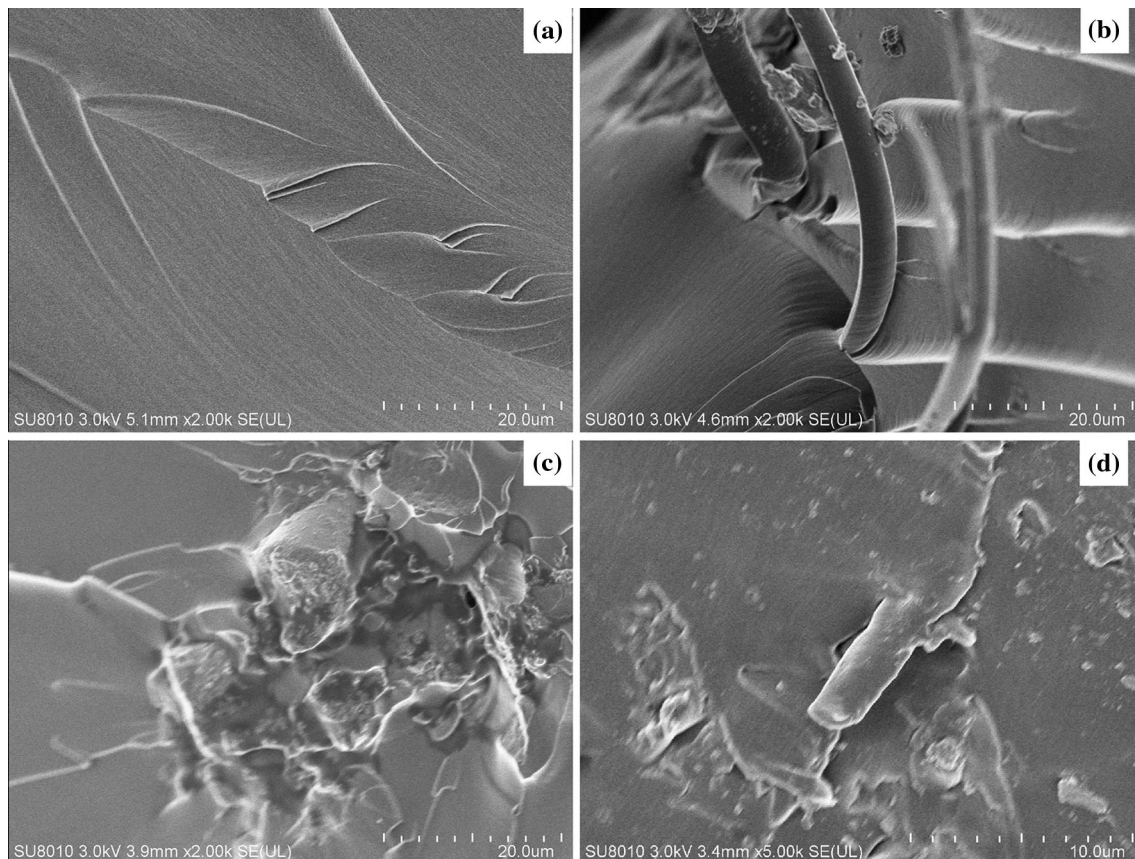


Fig. 10 FESEM morphologies of the impact fracture surfaces of neat epoxy (a), composites with GFs (b), and 2 wt% GF-ATHBPs (c, d)

Acknowledgements The authors gratefully acknowledge the supports from the National Natural Science Foundation of China (51202211 and 51402251), the National Science and Technology Major Project of the Ministry of Science and Technology of China (2012ZX04010032), the Natural science fund of Jiangsu Province (BK20130428), and the Research fund of Key Laboratory for Advanced Technology in Environmental Protection of Jiangsu Province (AE201111).

References

- Zaioncz S, Silva AA, Sirqueira AS, Soares BG (2007) Toughening of Epoxy resin by methyl methacrylate/2-ethylhexyl acrylate copolymers: the effect of copolymer composition. *Macromol Mater Eng* 292(12):1263–1270
- Liu Y, Zhang W, Zhou H (2005) Mechanical properties of epoxy resin/hydroxyl-terminated polyester blends: effect of two-phase structure. *Polym Int* 54(10):1408–1415
- Park J-S, Park S-S, Lee S (2007) Thermal and mechanical properties of carbon fiber reinforced epoxy composites modified with CTBN and hydroxyl terminated polyester. *Macromol Symp* 249–250(1):568–572
- Xu G, Gong M, Shi W (2005) Effects of hyperbranched poly(ester-silane) as a coupling agent on the mechanical behavior of glass bead filled epoxy resin. *Polym Adv Technol* 16(6):473–479
- Mezzenga R, Boogh L, Månson J-AE (2001) A review of dendritic hyperbranched polymer as modifiers in epoxy composites. *Compos Sci Technol* 61(5):787–795
- Punchaipetch P, D'Souza NA, Brostow W, Smith JT (2002) Mechanical properties of glass fiber composites with an epoxy resin modified by a liquid crystalline epoxy. *Polym Compos* 23(4):564–573
- Bozkurt E, Kaya E, Tanoglu M (2007) Mechanical and thermal behavior of non-crimp glass fiber reinforced layered clay/epoxy nanocomposites. *Compos Sci Technol* 67(15–16):3394–3403
- Xu Y, Van Hoa S (2008) Mechanical properties of carbon fiber reinforced epoxy/clay nanocomposites. *Compos Sci Technol* 68(3–4):854–861
- Kumar MA, Reddy KH, Reddy YVM, Reddy GR, Naidu SV (2010) Improvement of tensile and flexural properties in epoxy/clay nanocomposites reinforced with weave glass fiber reel. *Int J Polym Mater* 59(11):854–862
- Liu HX, Gu YZ, Li M, Zhang ZG (2012) Characterization of interfacial toughness in carbon fiber/epoxy resin composite subjected to water aging using single-fiber fragmentation method in an energy-based model. *Polym Compos* 33(5):716–722
- Masoodi R, El-Hajjar RF, Pillai KM, Sabo R (2012) Mechanical characterization of cellulose nanofiber and bio-based epoxy composite. *Mater Des* 36:570–576
- Naito K, Yang JM, Kagawa Y (2012) Tensile properties of high strength polyacrylonitrile (PAN)-based and high modulus pitch-based hybrid carbon fibers-reinforced epoxy matrix composite. *J Mater Sci* 47(6):2743–2751. doi:10.1007/s10853-011-6101-8
- Tehrani M, Boroujeni AY, Hartman TB, Haugh TP, Case SW, Al-Haik MS (2013) Mechanical characterization and impact damage assessment of a woven carbon fiber reinforced carbon nanotube-epoxy composite. *Compos Sci Technol* 75:42–48

14. Wu ZX, Li JW, Huang CJ, Huang RJ, Li LF (2013) Effect of gamma irradiation on the mechanical behavior, thermal properties and structure of epoxy/glass-fiber composite. *J Nucl Mater* 441(1–3):67–72
15. Rahmanian S, Suraya AR, Shazed MA, Zahari R, Zainudin ES (2014) Mechanical characterization of epoxy composite with multiscale reinforcements: carbon nanotubes and short carbon fibers. *Mater Des* 60:34–40
16. Strakhov IS, Rodnaya AI, Mezhevov YO, Korshak YV, Vagramyan TA (2014) Enhancement of the strength of a composite material based on ED-20 epoxy resin by reinforcement with a carbon fiber modified by electrochemical deposition of poly(*o*-phenylenediamine). *Russ J Appl Chem* 87(12):1918–1922
17. Withers GJ, Yu Y, Khabashesku VN, Cercone L, Hadjiev VG, Souza JM, Davis DC (2015) Improved mechanical properties of an epoxy glass-fiber composite reinforced with surface organomodified nanoclays. *Compos B Eng* 72:175–182
18. Eskizeybek V, Avci A, Gulce A (2014) The Mode I interlaminar fracture toughness of chemically carbon nanotube grafted glass fabric/epoxy multi-scale composite structures. *Compos A Appl Sci Manufact* 63:94–102
19. Boon MS, Saw WPS, Mariatti M (2012) Magnetic, dielectric and thermal stability of Ni–Zn ferrite-epoxy composite thin films for electronic applications. *J Magn Magn Mater* 324(5):755–760
20. Zhou W, Cai J (2012) Mechanical and dielectric properties of epoxy resin modified using reactive liquid rubber (HTPB). *J Appl Polym Sci* 124(5):4346–4351
21. Xiong X, Chen P, Zhang J, Yu Q, Wang B (2011) Preparation and properties of high performance phthalide-containing bismaleimide modified epoxy matrices. *J Appl Polym Sci* 121(6):3122–3130
22. An F, Lu CX, Li YH, Guo JH, Lu XX, Lu HB, He SQ, Yang Y (2012) Preparation and characterization of carbon nanotube-hybridized carbon fiber to reinforce epoxy composite. *Mater Des* 33:197–202
23. Fujiki K, Sakamoto M, Yoshikawa S, Sato T, Tsubokawa N (1998) Surface grafting of hyperbranched dendritic polymer onto glass fiber. *Compos Interfaces* 6(3):215–226
24. Venkateshwaran N, Perumal AE, Arunsundaranayagam D (2013) Fiber surface treatment and its effect on mechanical and visco-elastic behaviour of banana/epoxy composite. *Mater Des* 47:151–159
25. Liu T-M, Zheng Y-S, Hu J (2010) Surface modification of Aramid fibers with new chemical method for improving interfacial bonding strength with epoxy resin. *J Appl Polym Sci* 118(5):2541–2552
26. Guo JH, Lu CX, An F (2012) Effect of electrophoretically deposited carbon nanotubes on the interface of carbon fiber reinforced epoxy composite. *J Mater Sci* 47(6):2831–2836. doi:10.1007/s10853-011-6112-5
27. Ge HY, Ma XL, Liu HS (2015) Preparation of emulsion-type thermotolerant sizing agent for carbon fiber and the interfacial properties of carbon fiber/epoxy resin composite. *J Appl Polym Sci*. doi:10.1002/app.41882
28. Lin SP, Han JL, Yeh JT, Chang FC, Hsieh KH (2007) Surface modification and physical properties of various UHMWPE-fiber-reinforced modified epoxy composites. *J Appl Polym Sci* 104(1):655–665
29. Zhang Y, Huang Y, Liu L, Wu L (2007) Surface modification of aramid fibers with γ -ray radiation for improving interfacial bonding strength with epoxy resin. *J Appl Polym Sci* 106(4):2251–2262
30. Fu Y, Liu H, Zhong WH (2010) Wetting characteristics of epoxy resins modified by graphitic nanofibers with different functional groups. *Colloids Surf A* 369(1–3):196–202
31. Kamae T, Drzal LT (2012) Carbon fiber/epoxy composite property enhancement through incorporation of carbon nanotubes at the fiber–matrix interphase—part I: the development of carbon nanotube coated carbon fibers and the evaluation of their adhesion. *Compos A Appl Sci Manuf* 43(9):1569–1577
32. Chen YX, Zhou XD, Yin XC, Lin QF, Zhu MQ (2014) A novel route to modify the interface of glass fiber-reinforced epoxy resin composite via bacterial cellulose. *Int J Polym Mater Polym Biomater* 63(4):221–227
33. Liu WB, Zhang S, Li BC, Yang F, Jiao WC, Hao LF, Wang RG (2014) Improvement in interfacial shear strength and fracture toughness for carbon fiber reinforced epoxy composite by fiber sizing. *Polym Compos* 35(3):482–488
34. Buonocore GG, Schiavo L, Attianese I, Borriello A (2013) Hyperbranched polymers as modifiers of epoxy adhesives. *Compos B Eng* 53:187–192
35. Li S, Cui C, Hou H (2015) Synthesis of core–shell particles based on hyperbranched polyester and zirconium slag nanoparticles and its influence on the impact resistance of epoxy resin thermosets. *Polym Compos*. doi:10.1002/pc.23602
36. Li S, Cui C, Hou H (2015) Synthesis and characterization of amino-terminated hyperbranched polymer and as modifier for epoxy resin thermosets. *Colloid Polym Sci* 293:2681–2688
37. Li S, Cui C, Hou H, Wu Q, Zhang S (2015) The effect of hyperbranched polyester and zirconium slag nanoparticles on the impact resistance of epoxy resin thermosets. *Compos B Eng* 79:342–350
38. Luo L, Meng Y, Qiu T, Li X (2013) An epoxy-ended hyperbranched polymer as a new modifier for toughening and reinforcing in epoxy resin. *J Appl Polym Sci* 130(2):10
39. Foix D, Yu Y, Serra A, Ramis X, Salla JM (2009) Study on the chemical modification of epoxy/anhydride thermosets using a hydroxyl terminated hyperbranched polymer. *Eur Polymer J* 45(5):1454–1466
40. Morell M, Ramis X, Ferrando F, Yu Y, Serra A (2009) New improved thermosets obtained from DGEBA and a hyperbranched poly(ester-amide). *Polymer* 50(23):5374–5383
41. Fernández-Francos X, Foix D, Serra A, Salla JM, Ramis X (2010) Novel thermosets based on DGEBA and hyperbranched polymers modified with vinyl and epoxy end groups. *React Funct Polym* 70(10):798–806
42. Xiao X, Lu S, Qi B, Zeng C, Yuan Z, Yu J (2014) Enhancing the thermal and mechanical properties of epoxy resins by addition of a hyperbranched aromatic polyamide grown on microcrystalline cellulose fibers. *RSC Adv* 4(29):14928–14935
43. Wang R, Li Z, Wang Y, Liu W, Deng L, Jiao W, Yang F (2013) Effects of modified attapulgite on the properties of attapulgite/epoxy nanocomposites. *Polym Compos* 34(1):22–31